

Article

# Oxidation of Cefalexin by Permanganate: Reaction Kinetics, Mechanism, and Residual Antibacterial Activity

Yajie Qian <sup>1</sup>, Pin Gao <sup>1</sup>, Gang Xue <sup>1</sup>, Zhenhong Liu <sup>1</sup> and Jiabin Chen <sup>2,\*</sup>

<sup>1</sup> College of Environmental Science and Engineering, Donghua University, Shanghai 201620, China; yqian@dhu.edu.cn (Y.Q.); pingao@dhu.edu.cn (P.G.); xuegang@dhu.edu.cn (G.X.); zhhl@dhu.edu.cn (Z.L.)

<sup>2</sup> School of Environmental Science and Engineering, Suzhou University of Science and Technology, Suzhou 215009, China

\* Correspondence: chenjiabincn@163.com; Tel.: +86-0512-6809-6895

Received: 23 July 2018; Accepted: 8 August 2018; Published: 13 August 2018



**Abstract:** The oxidation of cefalexin (CFX), a commonly used cephalosporin antibiotic, was investigated by permanganate (PM) in water. Apparent second-order rate constant of the reaction between CFX and PM was determined to be  $12.71 \pm (1.62) \text{ M}^{-1} \cdot \text{s}^{-1}$  at neutral pH. Lower pH was favorable for the oxidation of CFX by PM. The presence of  $\text{Cl}^-$  and  $\text{HCO}_3^-$  could enhance PM-induced oxidation of CFX, whereas HA had negligible effect on CFX oxidation by PM. PM-induced oxidation of CFX was also significant in the real wastewater matrix. After addition of bisulfite (BS), PM-induced oxidation was significantly accelerated owing to the generation of Mn(III) reactive species. Product analysis indicated oxidation of CFX to three products, with two stereoisomeric sulfoxide products and one di-ketone product. The thioether sulfur and double bond on the six-membered ring were the reactive sites towards PM oxidation. Antibacterial activity assessment indicated that the activity of CFX solution was significantly reduced after PM oxidation.

**Keywords:** permanganate; water treatment; cefalexin; oxidation; product; antibacterial activity

## 1. Introduction

The  $\beta$ -lactam antibiotics, including penicillins and cephalosporins, are among the most extensively used antibiotics in human and veterinary medicine [1]. After consumption, a large portion of the administered dosages are excreted unchanged, thus a substantial amount of  $\beta$ -lactam antibiotics is expected to be released into the environment. Because  $\beta$ -lactam antibiotics developed at early stage, e.g., penicillin G, are susceptible to acid/ $\beta$ -lactamase catalyzed hydrolysis, their occurrence in the environment is scarcely reported. However, with the development of pharmacology, some  $\beta$ -lactam antibiotics are designed to be acid-stable and  $\beta$ -lactamase resistant, thus they are frequently detected in the environment [2]. For example, cefalexin (CFX), one of the most frequently used first generation cephalosporins, is relatively stable in aquatic environments. It has been widely detected in different water matrices, such as wastewater, surface water and even coastal water with the concentration up to  $\mu\text{g} \cdot \text{L}^{-1}$  [3–5]. The residual antibiotics in the environment could lead to adverse effects on non-target organisms, pose risk to drinking water supplies and increase the bacterial resistance [6]. Cephalosporins have the most prevalence of antibacterial resistance in pathogens according to the WHO 2014 report on antimicrobial resistance surveillance [7]. Therefore, it is imperative to develop effective strategies to eliminate CFX in the water environment.

Chemical oxidation processes involving permanganate (PM,  $\text{Mn(VII)}$ ) are promising technologies for eliminating contaminants in the water environment. Compared with other conventional oxidation processes, PM oxidation process is relatively cost-effective and less likely to generate disinfection

byproducts [8]. As an oxidant, PM exhibits a relatively high redox potential (i.e.,  $E_0 = 0.59\text{--}1.68\text{ V}$ ) and is effective for oxidizing a variety of inorganic and organic compounds, such as dissolved iron and manganese, odors and pharmaceuticals [9,10]. PM is always regarded as a selective oxidizing agent which exhibits highly variable rates to various contaminants. Generally, the second-order reaction rate constants between PM and organic contaminants are the range of  $10^{-5}\text{--}10^3\text{ M}^{-1}\cdot\text{s}^{-1}$  [11,12], which are relatively lower than those for the hydroxyl or sulfate radicals based oxidation ( $k''$ ,  $10^9\text{--}10^{10}\text{ M}^{-1}\cdot\text{s}^{-1}$ ). Recently, Sun et al. reported that the activation of PM by bisulfite (BS) can significantly enhance the oxidation of organic contaminants [13] and Mn(III) is deemed as the major reactive species involved in the oxidation process. However, it is still unclear whether PM exhibits reactivity towards CFX. As discussed below, PM was found to show considerable reactivity towards CFX, and the presence of BS could significantly enhance PM-induced oxidation of CFX.

As an oxidant, PM is expected to react with the moieties with available electrons during the oxidation of organic contaminants. In the molecular structure of CFX, the primary amine, and the thioether sulfur and double bond on the six-membered ring are electron-rich moieties, and thus they are potentially susceptible to electrophilic attack by the oxidants and lose electrons in the reaction. For example, the phenylglycine primary amine are the potentially reactive sites in the oxidation of CFX by Cu(II) [1] and ferrate(VI) [14]. The thioether sulfur on the six-membered ring was reported to be reactive to peroxymonosulfate [15] and sulfate radicals [16], while the double bond on the ring is susceptible to ozone oxidation [2]. The reactivity of PM with the above electron-rich moieties are still unknown, thus need to be further evaluated. Although CFX is susceptible to oxidative degradation by different oxidants, the products might still exhibit antibacterial activity, and thus pose potential risk to aquatic environment [17]. For example, biologically active products were found to be generated in the reactions of PG and CFX with ozone [2]. Ferrate(VI) oxidation is effective to lower the antibacterial activities of  $\beta$ -lactams, but  $\sim 24\%$  residual activity is still retained for the treated CFX [14]. Advanced oxidation processes (AOPs) are among the most effective processes for destroying micro-pollutants. The increase of antibacterial activities is reported in the hydroxyl radical-based AOPs treated water samples, such as UV/ $\text{H}_2\text{O}_2$  and photo-Fenton processes [18,19]. Therefore, it is essential to evaluate the antibacterial activity of the transformation products of CFX by PM oxidation.

In this work, we investigated the oxidation of CFX by PM. The objectives were: (1) to investigate the reactivity of PM towards CFX, and determine their reaction kinetics; (2) to evaluate the impact of reaction parameters and water matrices on PM-induced oxidation of CFX, and then assess the promoting effect of BS on CFX oxidation by PM; and (3) to identify the reactive sites on CFX towards PM oxidation, and then evaluate the antibacterial activity of the transformation products. As CFX shares the basic structure with other cephalosporin antibiotics, the findings of this work can provide important references for other cephalosporin antibiotics oxidation by PM.

## 2. Results and Discussion

### 2.1. Oxidation of CFX by PM

CFX possesses several electron-rich moieties, e.g., double bond and thioether sulfur on the six-membered ring, thus it is potentially reactive towards oxidants, such as PM. Indeed, rapid oxidation of CFX was observed when PM was present in the solution. For example, CFX was stable at neutral pH condition, but was almost completely degraded within 480 s after addition of 400  $\mu\text{M}$  PM (Figure 1). The oxidation of CFX followed the pseudo first-order kinetics, with the linear relationship ( $R^2$ ) higher than 0.995. The observed first-order rate constant ( $k_{obs}$  in Equation (1)) was calculated to be  $0.005\text{ s}^{-1}$ . The effect of PM concentrations on CFX oxidation was further evaluated at pH 7.0. The results showed that CFX oxidation increased when PM/CFX ratio increased from 5 to 30 (Figure 1A). The degradation of CFX followed first-order kinetics at different concentrations of PM, and the  $k_{obs}$  values increased from 0.002 to  $0.014\text{ s}^{-1}$  as the ratio increased from 5 to 30. The  $\log(k_{obs})$  was linearly increased with  $\log(C_{PM}/C_{CFX})$ , with the slope close to 1. Hence,  $k_{obs}$  was first-order with respect to PM

concentration. Apparent second-order rate constant ( $k_{2,app}$  in Equation (2)) was subsequently calculated to be  $12.71 \pm (1.62) \text{ M}^{-1} \cdot \text{s}^{-1}$  by dividing  $k_{obs}$  by the concentration of PM. The obtained  $k_{2,app}$  value of CFX with PM was comparable to those with peroxymonosulfate [15], but was smaller than those with ozone [2], ferrate(VI) [14] and radical species, e.g., sulfate radicals [20].

$$-\frac{d[\text{CFX}]}{dt} = k_{obs} \times [\text{CFX}] \quad (1)$$

$$-\frac{d[\text{CFX}]}{dt} = k_{2,app} \times [\text{CFX}] \times [\text{PM}] \quad (2)$$

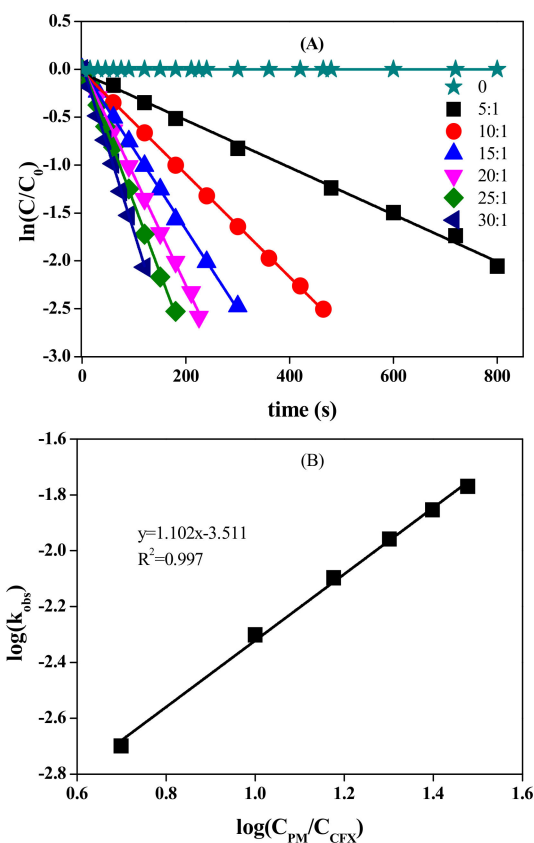


**Figure 1.** Effect of PM concentration on the oxidation of CFX (A), and  $\log(k_{obs})$  vs.  $\log(C_{PM}/C_{CFX})$  (B).  $[\text{CFX}] = 40 \mu\text{M}$ , pH 7.0. Note: the ratio is PM/CFX.

## 2.2. Effects of pH

The solution pH has been regarded as an important factor influencing oxidation of various organic contaminants by PM. Hence, the impact of pH was examined for PM-induced oxidation of CFX at pH 5.0–9.0, with the result shown in Figure 2. The oxidation of CFX by PM was pH dependent, and lower pH was favorable for PM-induced oxidation of CFX. Specifically, the  $k_{obs}$  of CFX gradually decreased from 0.006 to  $0.0041 \text{ s}^{-1}$  when pH increased from 5 to 9. Generally, the redox potential of PM decreased with increasing pH, i.e., acidic pH was favorable for enhancing the oxidation capacity of PM [21]. Hence, the faster oxidation of CFX by PM at lower pH might be attributed to the higher oxidation capacity of PM. This result was consistent with the previous reports that PM-induced oxidation of diclofenac decreased with the elevated pH [22]. However, the oxidative reactivity of PM with some contaminants, e.g., lincomycin and sulfamethoxazole, increased at elevated pH [23,24], whereas the oxidation of dichlorvos by PM was found to be unaffected by the solution pH [25]. Hence, pH impact

on PM-induced oxidation of organic contaminants was complicated, which was not only dependent on the oxidation capacity of PM, but also on the structure of target contaminants.

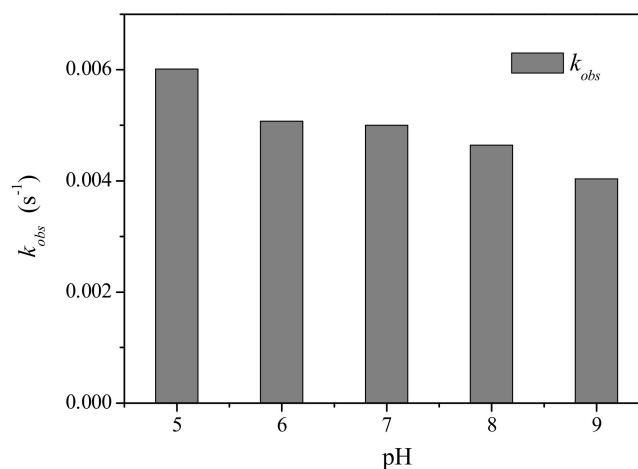


**Figure 2.** Effect of pH on the  $k_{obs}$  of CFX by PM oxidation.  $[CFX]_0 = 40 \mu M$ ,  $[PM]_0 = 400 \mu M$ .

The pH-dependent reactivity of PM towards contaminants was always related to the  $pK_a$  value of contaminants. For example, the reactivity of PM towards bisphenol A (BPA) was significantly dependent on pH when the solution pH was close to the  $pK_a$  value of BPA [26]. When the solution pH was far away from the  $pK_a$  value of carbamazepine (CBZ), the reactivity of PM towards CBZ was almost unaffected by the pH variation [26]. pH could affect the protonation/deprotonation of some functional group, e.g., primary amine, and thus influenced its electron density and susceptibility to PM oxidation. The  $pK_{a2}$  of CFX is 6.86, thus the primary amine on the side chain of CFX was deprotonated at alkaline pHs and possesses higher electron density than the protonated ones at pH 5. If primary amine was the reactive site on CFX, faster degradation of CFX by PM could be expected at alkaline pHs, which was opposite to the results in this work. Therefore, the primary amine on the side chain might be not the reactive site for PM oxidation, which is further elucidated in the following sections.

### 2.3. Effects of Water Matrices

The water matrices, e.g., the inorganic and organic solute, might affect the oxidation of target organic contaminants during PM oxidation. Hence, we further evaluated the effect of common ions, e.g.,  $Cl^-$  and  $HCO_3^-$ , on PM-induced CFX oxidation. As shown in Figure 3A, the calculated  $k_{obs}$  of CFX oxidation increased with the increasing concentration of  $Cl^-$  from 0 to 500 mM. Similarly, the presence of  $HCO_3^-$  promoted the oxidation of CFX by PM, and the rate constants also increased when  $HCO_3^-$  concentrations increased from 0 to 50 mM (Figure 3B). This result was consistent with a previous report that the common ions, e.g.,  $HCO_3^-$ , exhibited strong accelerating effect on BPA oxidation by PM, but the mechanism was still ambiguous and need further investigation [27].

We further investigated the impact of HA on the oxidation of CFX by PM, and the result showed that PM-induced oxidation of CFX was not affected by various concentrations of HA (Figure 3C). As a common matrix in the real waters, the effect of HA on PM-induced oxidation of organic contaminants have been extensively evaluated, and its impact was complicated. HA was regarded as a reductant to inhibit the oxidation of SMX by PM [23], whereas it was also reported to promote the oxidation of some organic contaminants when the concentration of HA was lower than PM [28]. In some previous reports, the impact of HA on the oxidation of contaminants were dependent on HA concentration and source. For example, HA could accelerate the oxidation of phenol by PM when low concentration of HA was present in the solution, but gradually inhibited phenol oxidation as HA concentration increased [29]. At the constant concentration of HA, commercial HA and HA extracted from soils exhibited different impact on the contaminant degradation, which could be attributed to their different

functional groups [30]. In another study, HA also exhibited negligible effect on the PM-induced oxidation of contaminants [9], which was consistent with the result in this work. Although the examined HA exhibited negligible effect, a wider diversity of HA sources need to be evaluated on whether HA influences reaction between CFX with PM [27].

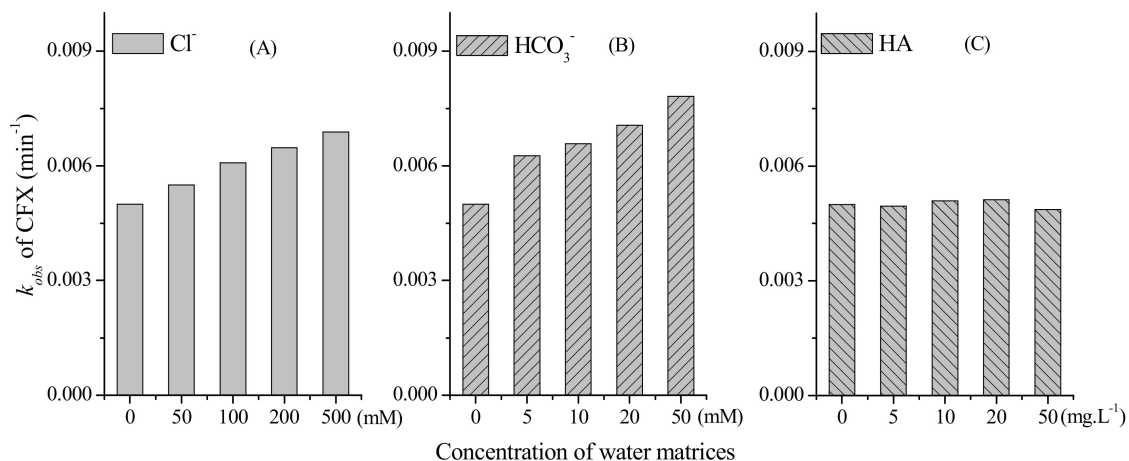


**Figure 3.** Degradation rate constants ( $k_{obs}$ ) of CFX under different concentration of: (A) Cl<sup>-</sup>; (B) HCO<sub>3</sub><sup>-</sup>; and (C) NOM. [CFX]<sub>0</sub> = 40  $\mu\text{M}$ , [PM]<sub>0</sub> = 400  $\mu\text{M}$ , pH 7.

PM-induced oxidation of CFX was also evaluated in the real water sample. Four hundred micromolars of PM and 0.2  $\mu\text{M}$  of CFX were spiked into wastewater (WW) sample (water quality is shown in Table S1), which was maintained at pH 7 with PB (10 mM). Before spiking, CFX was confirmed to be negligible in the WW sample. Results showed that significant degradation of CFX was observed in WW without addition of PM (Figure S1). The  $\beta$ -lactam ring in CFX was susceptible to breakage catalyzed by metal ions, alkali and other water matrices [0], hence CFX degradation in WW was significant even without spiking PM. After addition of PM, the degradation of CFX was significantly enhanced, and PM-induced degradation of CFX in WW was slightly slower than that in the DI water (Figure S1). In the real WW sample, although the anions, e.g., HCO<sub>3</sub><sup>-</sup> and Cl<sup>-</sup>, could promote PM-induced oxidation of CFX, the water matrix, e.g., reduced substances, might also consume PM, thus lowering the degradation of CFX by PM. Overall, PM-induced oxidation of CFX was significant in the real wastewater matrix, and thus PM was an efficient oxidant to eliminate CFX in the real WW samples.

#### 2.4. Impact of BS on PM-Induced Oxidation of CFX

BS has been reported to significantly accelerate the oxidation of organic contaminants, e.g., phenol, by PM. Hence, we further evaluated the oxidation of CFX in the PM/BS system. As shown in Figure S2, degradation of CFX was negligible in the presence of 600  $\mu\text{M}$  BS alone, while about 30% of CFX was degraded within 15 min by 80  $\mu\text{M}$  PM. However, complete degradation of CFX was achieved within 10 min in the combination of PM and BS. The results indicated that PM and BS had synergistic effect on the oxidation of CFX. Indeed, BS was regarded as an efficient activator for PM to generate a reactive intermediate, i.e., Mn(III), which could oxidize organic contaminants at an extremely rapid rate. In PM/BS system, the rapid oxidation of CFX was also likely induced by the reactive Mn(III) generated from the reduction of PM by BS.

The impact of different dosages of PM and BS on the oxidation of CFX was further investigated (Figure 4A). In the absence of BS, the oxidation of CFX increased from 4% to 65% after 20 min when PM dosage increased from 2  $\mu\text{M}$  to 80  $\mu\text{M}$  (Figure S3). In the presence of 600  $\mu\text{M}$  BS, CFX oxidation increased from 35% to 75% after 20 min with the increasing dosage of PM from 2  $\mu\text{M}$  to 20  $\mu\text{M}$ . Complete degradation of CFX could be achieved when PM further increased to 40  $\mu\text{M}$ . However, the degradation

of CFX could not be further enhanced when PM increased to 80  $\mu\text{M}$ . With the increasing dosage of PM, more Mn(III) reactive species could be generated to oxidize CFX. When high dosage of PM was present, PM could consume the Mn(III), thus the degradation of contaminant could not be further increased.

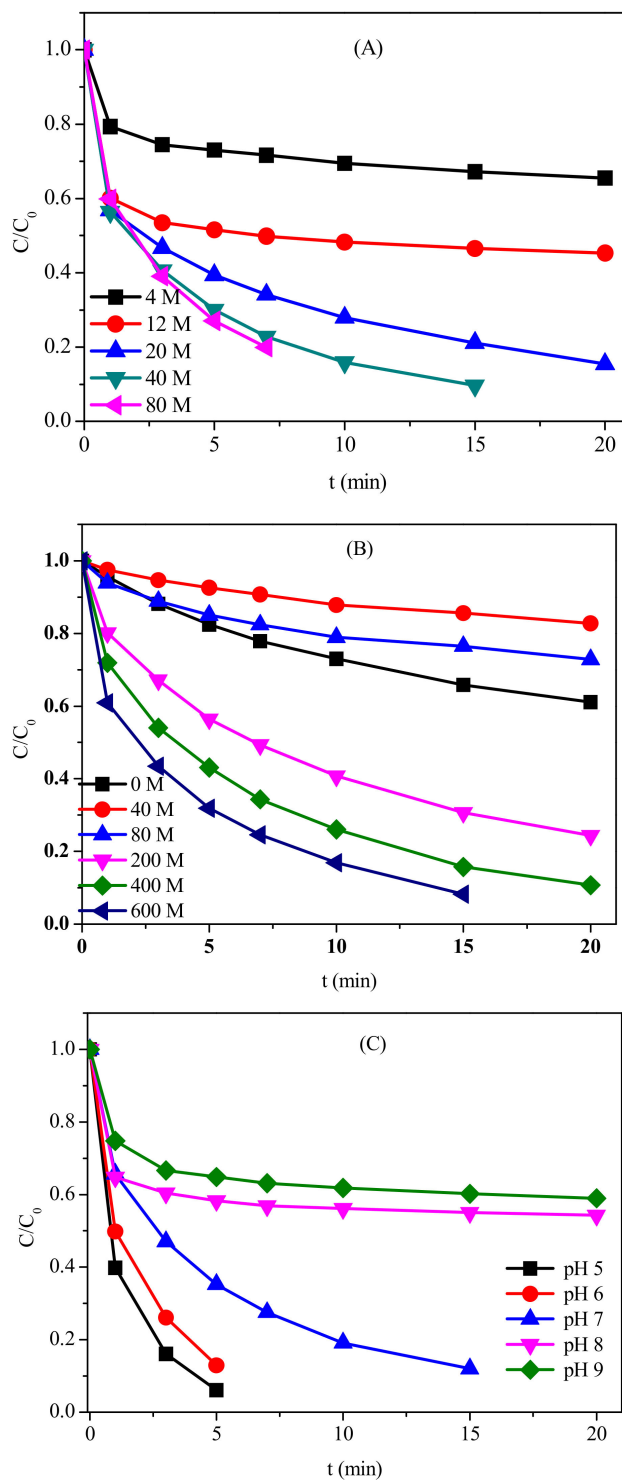


**Figure 4.** Effect of PM concentrations (A); BS dosages (B); and pH (C) on the oxidation of CFX in PM/BS system.  $[\text{CFX}]_0 = 40 \mu\text{M}$ ; (A)  $[\text{BS}]_0 = 600 \mu\text{M}$ , pH = 7; (B)  $[\text{PM}]_0 = 40 \mu\text{M}$ , pH = 7; and (C)  $[\text{PM}]_0 = 40 \mu\text{M}$ ,  $[\text{BS}]_0 = 600 \mu\text{M}$ .

Compared to the impact of PM concentration, effect of BS concentration on the oxidation of CFX was more complicated. In the presence of 40  $\mu\text{M}$  PM, the oxidation of CFX was slightly inhibited in the presence of low BS dosage, but was significantly promoted when high concentration of BS was present (Figure 4B). For example, the degradation efficiency of CFX within 20 min decreased from 39% (PM alone) to 17% and 25% when 40  $\mu\text{M}$  and 80  $\mu\text{M}$  BS were present, respectively. However, almost complete degradation of CFX was achieved within 20 min and 15 min in the presence of 400  $\mu\text{M}$  and 600  $\mu\text{M}$  BS, respectively. When low concentration of BS was present in PM/BS system, the generated Mn(III) could be consumed by PM, thus reducing the effective oxidants (i.e., PM and Mn(III)) responsible for CFX degradation. When the concentration of BS increased to 200  $\mu\text{M}$  or even higher, almost all PM was transformed to Mn(III), thus the reactive Mn(III) was the dominant oxidant in the reaction system.

pH also had a significant impact on CFX oxidation in PM/BS system. As shown in Figure 4C, CFX degradation was rapid at pH 5.0 and decreased as pH increased from 5.0 to 9.0. As the generated Mn(III) is unstable and prone to disproportionate under alkaline conditions [13], higher pH was unfavorable for the oxidation of CFX in PM/BS system. Furthermore, the speciation of BS is strongly influenced by solution pH ( $\text{HSO}_3^- \rightleftharpoons \text{SO}_3^{2-} + \text{H}^+$ ,  $\text{p}K_a = 7.2$ ), which will convert to less reactive sulfite under alkaline conditions [31]. Hence, acidic condition was favorable for CFX oxidation.

### 2.5. Product Analysis

To identify the potential reaction site of CFX towards PM oxidation, we subsequently analyzed the oxidation products of CFX by PM. Transformation products of CFX by PM were analyzed by LC/MS/MS. Two products with molecular weight (MW) of 363, and one product with MW of 379 were generated after oxidation of CFX (MW: 347) by PM (Figure S4–S6). The MW 363 ( $M + 16$ ) and 379 products ( $M + 32$ ) were likely generated via the addition of one or two oxygen atoms on the molecule of CFX, respectively. The two MW 363 products (363a and 363b) might be isomers since they have different LC retention time but similar MW and MS fragment patterns. The  $M + 16$  products were also previously reported as the main oxidation products of CFX by peroxymonosulfate [15], ozone [2], ferrate (VI) [14], and sulfate radical [32]. They were identified as stereoisomeric CFX-(R)-sulfoxide and CFX-(S)-sulfoxide. We subsequently analyzed the oxidation products of CFX by peroxymonosulfate with the analytical methods in this work. The result indicated that CFX-(R)-sulfoxide and CFX-(S)-sulfoxide generated by peroxymonosulfate matched the 363a and 363b products in LC retention time and MS fragment patterns. Hence, the 363a and 363b products were verified as CFX-(R)-sulfoxide and CFX-(S)-sulfoxide, respectively. Based on the MS spectrum, 379 product contains the fragment of  $m/z$  106, which is characterized by the intact primary amine moiety on the side chain. Hence, the two oxygen atoms were most likely added on the double bond on six membered ring, which was also proposed in the oxidation of CFX by ozone [2].

For the sulfoxide products, the thioether sulfur on the six-membered ring of CFX was the reaction site for PM oxidation. Indeed, the thioether sulfur was susceptible to oxidative transformation by various oxidants, e.g., peroxymonosulfate [15], ferrate(VI) [14] and sulfate radicals [32]. The CFX-sulfoxide products were generated by the electrophilic attack of the positively charged Mn atom in PM on the thioether sulfur to form Mn-sulfur intermediate 1. Subsequently, a pair of electrons of sulfur were donated to a d-orbital of Mn, inducing the formation of a coordinate covalent intermediate 2, which were further decomposed to sulfoxide products by rearrangement [33] (Figure 5, scheme 1). For the 379 product, the double bond on the six-membered ring was the reaction site for PM oxidation. The positively charged Mn electrophile attacked the unsaturated C=C bond on the ring, and then forming cyclic hypomanganate(V) ester (intermediate 3) via an activated organometallic complex. Afterwards, the cyclic manganite(VI) ester (intermediate 4) was generated from the cyclic hypomanganate(V) ester by the oxidation of PM, and subsequently hydrolyzed to generate di-ketone-containing product [33] (Figure 5, scheme 2).

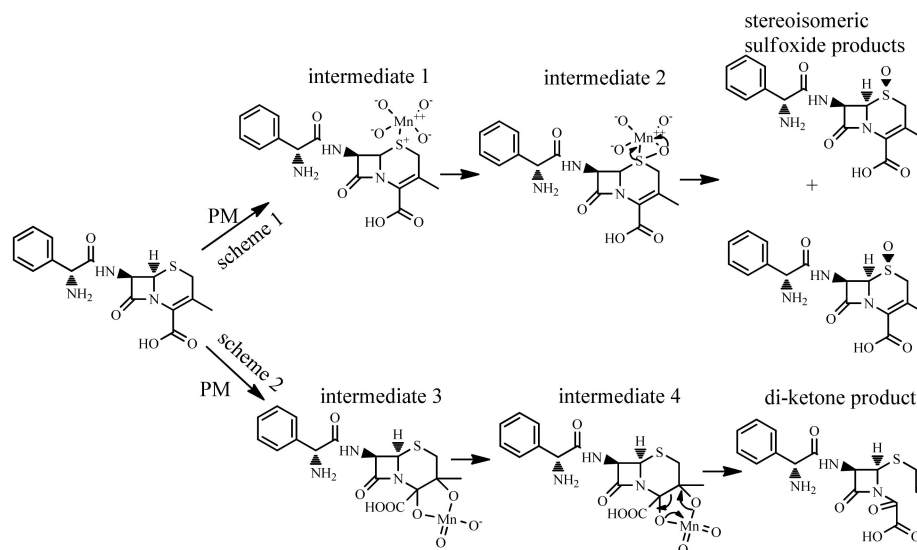


**Figure 5.** Transformation products of CFX by PM.

### 2.6. Antibacterial Activity Assessment

Although PM was effective to oxidize CFX, the  $\beta$ -lactam ring still existed in the transformation products. To investigate whether the products possess biological activity, we further evaluated the antibacterial activity of the transformation products of CFX by PM with *E. coli* as the tested bacteria. As shown in Figure 6, the growth of *E. coli* could be completely inhibited in the presence of 40  $\mu$ M CFX. After addition of PM, the antibacterial activity of CFX solution gradually decreased along with the gradual oxidation of CFX. Specifically, the growth inhibition was reduced to 13% after 8 min when about 92% of initial CFX was oxidatively degraded in the presence of PM. This result indicated that the biological activity of CFX could be significantly reduced after treatment of PM. Various oxidants have been investigated to remove the antibacterial activity of CFX. For example, peroxydisulfate [15], ozone [34] and ferrate(VI) [14] were found to significantly eliminate the biological activity of CFX. However, the products of  $\beta$ -lactam antibiotics (e.g., AMX) with UV/TiO<sub>2</sub> still exhibited significant activity to *Enterococcus faecalis* (ATCC 14506). The results in this work indicated that PM was effective to eliminate the biological activity of CFX.

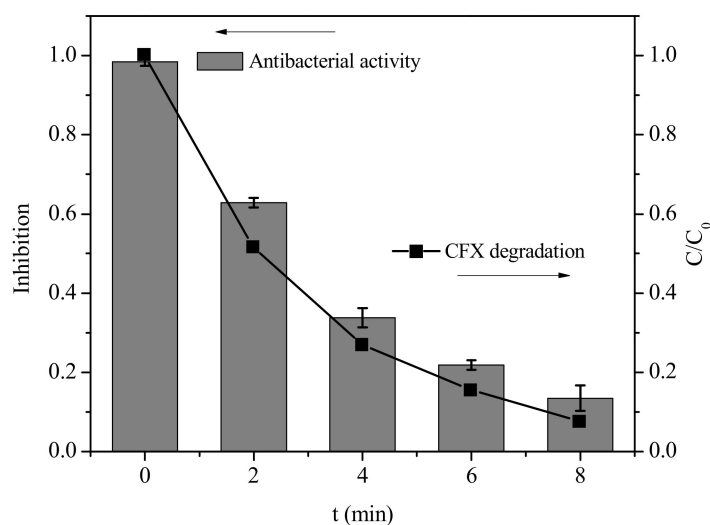


**Figure 6.** Growth inhibition of *Escherichia coli*. [CFX] = 40  $\mu$ M, [PM] = 400  $\mu$ M, and pH = 7 (10 mM PB). Error bars represent standard deviations of data from triplicate samples.

### 3. Materials and Methods

#### 3.1. Chemicals

Cefalexin (CFX,  $\geq 99\%$ ) was purchased from Sigma-Aldrich (St. Louis, MO, USA). Potassium permanganate (PM,  $\geq 99.5\%$ ) and sodium bisulfite (BS,  $\geq 99.9\%$ ) were obtained from Aladdin (Shanghai, China). The HPLC grade of phosphoric acid and methanol were obtained from Sigma-Aldrich. Humic acid (HA) was purchased from ANPEL Laboratory Technologies Inc. (Shanghai, China). Other chemicals and reagents used were in analytical grade or higher, and obtained from Sigma-Aldrich (St. Louis, MO, USA) or Aladdin (Shanghai, China). All chemicals were used as received without any further purification. Reagent grade deionized (DI) water was produced by a Milli-Q Ultrapure Gradient A10 purification system (Millipore, Burlington, MA, USA).

#### 3.2. Real Water Samples

Wastewater (WW) after biological treatment was sampled from a municipal wastewater treatment plant located in the south region of China. Samples were filtered through 0.45  $\mu\text{m}$  glass fiber filters and then stored under 4 °C before use. The water parameters of WW are present in Table S1.

#### 3.3. Experimental Setup

Batch experiments were conducted in 100 mL amber serum bottles open to the air. The reaction solution in the bottles were constantly mixed by a magnetic stirring. Except where mentioned, phosphate buffer (PB, 10 mM) was used to control the solution pH at 7. PM (400  $\mu\text{M}$ ) were added into the solution containing CFX (40  $\mu\text{M}$ ) and PB to initiate the reaction. The pre-determined concentration of  $\text{Cl}^-$ ,  $\text{HCO}_3^-$  or HA was added into the above reaction system to evaluate their impact on CFX degradation. BS (600  $\mu\text{M}$ ) was added in the solution containing PM (40  $\mu\text{M}$ ), CFX (40  $\mu\text{M}$ ), and PB to evaluate the effect of BS. To investigate the pH impact, the solution was controlled at pH 5–9 with 10 mM PB. Samples were periodically withdrawn and supplemented with excess sodium thiosulfate to quench reactive species. The quenched samples were stored at 2 mL amber vial at 4 °C and analyzed within 24 h. All experiments were conducted in duplicates or more.

#### 3.4. Analytical Methods

CFX was analyzed by an Agilent 1200 series HPLC system equipped with a UV diode-array detector (DAD). Samples were separated using a Zorbax Extend-C18 column (4.6  $\times$  250 mm, 5  $\mu\text{m}$ ) and detected at 262 nm. Isocratic elution was employed using 10 mM  $\text{H}_3\text{PO}_4$  solution and methanol (70:30, *v/v*) with a flow rate of 1 mL/min.

The transformation products were separated on HPLC system (Ultimate 3000, Dionex, Sunnyvale, CA, USA) with a C18 column (2.1  $\times$  150 mm, 5  $\mu\text{m}$ ), and analyzed with a triple quadrupole mass spectrometry (TSQ Quantum Ultra EMR, Thermo Fisher Scientific, Waltham, MA, USA). The mobile phase consisted of (A) 0.1% formic acid in water and (B) acetonitrile at a flow rate of 0.2 mL/min: 5% B was kept for 2 min, then ramped to 30% B over 10 min, kept for 10 min. The mass spectrometer was operated at positive electrospray ionization (ESI+). Then, product-full-scan mode was used to obtain sufficient fragment information for structure elucidation.

#### 3.5. Bacterial Growth Inhibition Bioassays

The antibacterial activity of CFX before and after treatment by PM was determined with *E. coli* (ATCC 25,922) as reference strains. Briefly, 4 mL aliquots were taken at the predetermined time (i.e., 0, 2, 4, 6, and 8 min), and immediately quenched by  $\text{Na}_2\text{S}_2\text{O}_3$ . Then, the sample was subsequently inoculated with 1 mL of a broth *E. coli* culture ( $1 \times 10^6$  CFU  $\text{mL}^{-1}$ ), which was incubated overnight in sterile Mueller–Hinton broth at 37 °C. The samples were further incubated for 8 h at 37 °C on a shaking incubator rotating at 170 rpm. Control experiments with  $\text{Na}_2\text{S}_2\text{O}_3$  or DI water dosing 1 mL of

*E. coli* broth culture were also conducted. The growth of *E. coli* was found to be unaffected by Na<sub>2</sub>S<sub>2</sub>O<sub>3</sub>. After the incubation, the bacterial growth was evaluated by determining the optical density (OD) at 625 nm on a UV-vis spectrophotometer (Mapada UV-1600 PC), and then comparing this value to the initial OD value of each sample. The OD value was subsequently converted to growth inhibition, I, according to

$$I = (A_0 - A)/A_0$$

where A<sub>0</sub> represents the maximum absorbance for control, which corresponds to uninhibited culture growth. The values of I vary from 0 (null inhibition) to 1 (complete inhibition). All experiments were performed in triplicates, and the results were reported as the mean with standard deviations.

#### 4. Conclusions

PM exhibits high performance in the oxidative degradation of CFX. Apparent second-order rate constant of the reaction between CFX and PM was calculated to be  $12.71 \pm 1.62 \text{ M}^{-1} \cdot \text{s}^{-1}$ . Lower pH was favorable for PM-induced oxidation of CFX. PM-induced CFX oxidation could be promoted in the presence of Cl<sup>-</sup> and HCO<sub>3</sub><sup>-</sup>, and the promoting effect increased with the increasing concentration of coexisted ions, whereas HA had no effect on the oxidation of CFX by PM. Oxidation of CFX by PM was also significant in the wastewater matrix. The presence of BS could significantly accelerate the oxidation of CFX by PM. Product analysis indicated that two products with MW of 363 and one product with MW of 379 were the primary products of CFX by PM oxidation. The thioether sulfur and double bond on the six-membered ring were proposed as the main reaction sites in CFX towards PM oxidation. The antibacterial activity of the transformation products was significantly reduced after treatment of CFX by PM. Therefore, PM oxidation was an effective approach to significantly eliminate CFX and its biological activity.

**Supplementary Materials:** The supplementary materials are available online.

**Author Contributions:** Y.Q. and J.C. conceived and designed the experiments; Y.Q. performed the experiments; P.G. and G.X. analyzed the data; Z.L. contributed reagents/materials/analysis tools; J.C. wrote the paper.

**Funding:** This work was supported by the Fundamental Research Funds for the Central Universities (NO. 2232018D3-08), National Science Foundation of China (No. 51708097 and 51509175), Natural Science Foundation of Shanghai (17ZR1400400) and China Postdoctoral Science Foundation (No. 2017M611422).

**Conflicts of Interest:** The authors declare no conflicts of interest.

#### References

1. Chen, J.B.; Sun, P.Z.; Zhang, Y.L.; Huang, C.H. Multiple roles of Cu(II) in catalyzing hydrolysis and oxidation of β-Lactam antibiotics. *Environ. Sci. Technol.* **2016**, *50*, 12156–12165. [[CrossRef](#)] [[PubMed](#)]
2. Dodd, M.C.; Rentsch, D.; Singer, H.P.; Kohler, H.P.E.; von Gunten, U. Transformation of β-Lactam antibacterial agents during aqueous ozonation: Reaction pathways and quantitative bioassay of biologically-active oxidation products. *Environ. Sci. Technol.* **2010**, *44*, 5940–5948. [[CrossRef](#)] [[PubMed](#)]
3. Minh, T.B.; Leung, H.W.; Loi, I.H.; Chan, W.H.; So, M.K.; Mao, J.Q.; Choi, D.; Lam, J.C.W.; Zheng, G.; Martin, M.; et al. Antibiotics in the Hong Kong metropolitan area: Ubiquitous distribution and fate in Victoria Harbour. *Mar. Pollut. Bull.* **2009**, *58*, 1052–1062. [[CrossRef](#)] [[PubMed](#)]
4. Chen, J.B.; Wang, Y.; Qian, Y.J.; Huang, T.Y. Fe(III)-promoted transformation of β-lactam antibiotics: Hydrolysis vs oxidation. *J. Hazard. Mater.* **2017**, *335*, 117–124. [[CrossRef](#)] [[PubMed](#)]
5. Li, S.; Shi, W.Z.; Liu, W.; Li, H.M.; Zhang, W.; Hu, J.R.; Ke, Y.C.; Sun, W.L.; Ni, J.R. A duodecennial national synthesis of antibiotics in China's major rivers and seas (2005–2016). *Sci. Total Environ.* **2018**, *615*, 906–917. [[CrossRef](#)] [[PubMed](#)]
6. Huang, T.Y.; Fang, C.; Qian, Y.J.; Gu, H.D.; Chen, J.B. Insight into Mn(II)-mediated transformation of β-lactam antibiotics: the overlooked hydrolysis. *Chem. Eng. J.* **2017**, *321*, 662–668. [[CrossRef](#)]
7. World Health Organization. *Antimicrobial Resistance: Global Report on Surveillance*; WHO Press: Geneva, Switzerland, 2014.

8. Crittenden, J.C.; Trussell, R.R.; Hand, D.W.; Howe, K.J.; Tchobanoglous, G. *MWH's Water Treatment: Principles and Design*; John Wiley & Sons: Hoboken, NJ, USA, 2012.
9. Hu, L.H.; Martin, H.M.; Arce-Bulted, O.; Sugihara, M.N.; Keating, K.A.; Strathmann, T.I. Oxidation of carbamazepine by Mn(VII) and Fe(VI): Reaction kinetics and mechanism. *Environ. Sci. Technol.* **2009**, *43*, 509–515. [[CrossRef](#)] [[PubMed](#)]
10. Jiang, J.; Pang, S.Y.; Ma, J. Oxidation of triclosan by permanganate (Mn(VII)): Importance of ligands and in situ formed manganese oxides. *Environ. Sci. Technol.* **2009**, *43*, 8326–8331. [[CrossRef](#)] [[PubMed](#)]
11. Waldemer, R.H.; Tratnyek, P. Kinetics of contaminant degradation by permanganate. *Environ. Sci. Technol.* **2006**, *40*, 1055–1061. [[CrossRef](#)] [[PubMed](#)]
12. Pang, S.Y.; Jiang, J.; Gao, Y.; Zhou, Y.; Huangfu, X.L.; Liu, Y.Z.; Ma, J. Oxidation of flame retardant tetrabromobisphenol A by aqueous permanganate: reaction kinetics, brominated products, and pathways. *Environ. Sci. Technol.* **2014**, *48*, 615–623. [[CrossRef](#)] [[PubMed](#)]
13. Sun, B.; Guan, X.H.; Fang, J.Y.; Tratnyek, P. Activation of manganese oxidants with bisulfite for enhanced oxidation of organic contaminants: The involvement of Mn(III). *Environ. Sci. Technol.* **2015**, *49*, 12414–12421. [[CrossRef](#)] [[PubMed](#)]
14. Karlesa, A.; De Vera, G.A.; Dodd, M.C.; Park, J.; Espino, M.P.B.; Lee, Y.H. Ferrate(VI) oxidation of  $\beta$ -Lactam antibiotics: Reaction kinetics, antibacterial activity changes, and transformation products. *Environ. Sci. Technol.* **2014**, *48*, 10380–10389. [[CrossRef](#)] [[PubMed](#)]
15. Chen, J.B.; Fang, C.; Xia, W.J.; Huang, T.Y.; Huang, C.H. Selective transformation of  $\beta$ -Lactam antibiotics by peroxymonosulfate: Reaction kinetics and nonradical mechanism. *Environ. Sci. Technol.* **2018**, *52*, 1461–1470. [[CrossRef](#)] [[PubMed](#)]
16. Zhou, X.F.; Liu, D.D.; Zhang, Y.L.; Chen, J.B.; Chu, H.Q.; Qian, Y.J. Degradation mechanism and kinetic modeling for UV/peroxydisulfate treatment of penicillin antibiotics. *Chem. Eng. J.* **2018**, *52*, 93–101. [[CrossRef](#)]
17. Zhang, R.C.; Yang, Y.K.; Huang, C.H.; Li, N.; Liu, H.; Zhao, L.; Sun, P.Z. UV/H<sub>2</sub>O<sub>2</sub> and UV/PDS treatment of trimethoprim and sulfamethoxazole in synthetic human urine: Transformation products and toxicity. *Environ. Sci. Technol.* **2016**, *50*, 2573–2583. [[CrossRef](#)] [[PubMed](#)]
18. Jung, Y.J.; Kim, W.G.; Yoon, Y.J.; Kang, J.W.; Hong, Y.M.; Kim, H.W. Removal of amoxicillin by UV and UV/H<sub>2</sub>O<sub>2</sub> processes. *Sci. Total Environ.* **2012**, *420*, 160–167. [[CrossRef](#)] [[PubMed](#)]
19. Trovó, A.G.; Pupo Nogueira, R.F.; Agüera, A.; Fernandez-Alba, A.R.; Malato, S. Degradation of the antibiotic amoxicillin by photo-Fenton process—chemical and toxicological assessment. *Water Res.* **2011**, *45*, 1394–1402. [[CrossRef](#)] [[PubMed](#)]
20. Rickman, K.A.; Mezyk, S.P. Kinetics and mechanisms of sulfate radical oxidation of  $\beta$ -lactam antibiotics in water. *Chemosphere* **2010**, *81*, 359–365. [[CrossRef](#)] [[PubMed](#)]
21. Lam, W.W.Y.; Man, W.L.; Leung, C.F.; Wong, C.Y.; Lau, T.C. Solvent effects on the Oxidation of Ru<sup>IV</sup>O to ORu<sup>VI</sup>O by MnO<sub>4</sub><sup>-</sup>. Hydrogen-atom versus oxygen-atom transfer. *J. Am. Chem. Soc.* **2007**, *129*, 13646–13652. [[CrossRef](#)] [[PubMed](#)]
22. Cheng, H.Y.; Song, D.; Liu, H.J.; Qu, J.H. Permanganate oxidation of diclofenac: The pH-dependent reaction kinetics and a ring-opening mechanism. *Chemosphere* **2015**, *136*, 297–304. [[CrossRef](#)] [[PubMed](#)]
23. Gao, S.S.; Zhao, Z.W.; Xu, Y.P.; Tian, J.Y.; Qi, H.; Lin, W.; Cui, F.Y. Oxidation of sulfamethoxazole (SMX) by chlorine, ozone and permanganate—A comparative study. *J. Hazard. Mater.* **2014**, *274*, 258–269. [[CrossRef](#)] [[PubMed](#)]
24. Hu, L.H.; Martin, H.M.; Strathmann, T.J. Oxidation kinetics of antibiotics during water treatment with potassium permanganate. *Environ. Sci. Technol.* **2010**, *44*, 6416–6422. [[CrossRef](#)] [[PubMed](#)]
25. Liu, C.; Qiang, Z.M.; Adams, C.; Tian, F.; Zhang, T. Kinetics and mechanism for degradation of dichlorvos by permanganate in drinking water treatment. *Water Res.* **2009**, *43*, 3435–3442. [[CrossRef](#)] [[PubMed](#)]
26. Jiang, J.; Pang, S.Y.; Ma, J. Role of ligands in permanganate oxidation of organics. *Environ. Sci. Technol.* **2010**, *44*, 4270–4275. [[CrossRef](#)] [[PubMed](#)]
27. Zhang, J.; Sun, B.; Guan, X.H. Oxidative removal of bisphenol A by permanganate: Kinetics, pathways and influences of co-existing chemicals. *Sep. Purif. Technol.* **2013**, *107*, 48–53. [[CrossRef](#)]
28. Jiang, J.; Pang, S.Y.; Ma, J.; Liu, H.L. Oxidation of phenolic endocrine disrupting chemicals by potassium permanganate in synthetic and real waters. *Environ. Sci. Technol.* **2012**, *46*, 1774–1781. [[CrossRef](#)] [[PubMed](#)]

29. He, D.; Guan, X.H.; Ma, J.; Yu, M. Influence of different nominal molecular weight fractions of humic acids on phenol oxidation by permanganate. *Environ. Sci. Technol.* **2009**, *43*, 8332–8337. [[CrossRef](#)] [[PubMed](#)]
30. He, D.; Guan, X.H.; Ma, J.; Yang, X.; Cui, C.W. Influence of humic acids of different origins on oxidation of phenol and chlorophenols by permanganate. *J. Hazard. Mater.* **2010**, *182*, 681–688. [[CrossRef](#)] [[PubMed](#)]
31. Tartar, H.V.; Garretson, H.H. The thermodynamic ionization constants of sulfurous acid at 25°. *J. Am. Chem. Soc.* **1941**, *63*, 808–816. [[CrossRef](#)]
32. Qian, Y.J.; Xue, G.; Chen, J.B.; Luo, J.M.; Zhou, X.F.; Gao, P.; Wang, Q. Oxidation of cefalexin by thermally activated persulfate: Kinetics, products, and antibacterial activity change. *J. Hazard. Mater.* **2018**, *354*, 153–160. [[CrossRef](#)] [[PubMed](#)]
33. Li, L.P.; Wei, D.B.; Wei, G.H.; Du, Y.G. Oxidation of cefazolin by potassium permanganate: Transformation products and plausible pathways. *Chemosphere* **2016**, *149*, 279–285. [[CrossRef](#)] [[PubMed](#)]
34. Dodd, M.C.; Kohler, H.P.E.; von Gunten, U. Oxidation of antibacterial compounds by ozone and hydroxyl radical: Elimination of biological activity during aqueous ozonation processes. *Environ. Sci. Technol.* **2009**, *43*, 2498–2504. [[CrossRef](#)] [[PubMed](#)]



© 2018 by the authors. Licensee MDPI, Basel, Switzerland. This article is an open access article distributed under the terms and conditions of the Creative Commons Attribution (CC BY) license (<http://creativecommons.org/licenses/by/4.0/>).